

Polymer Encapsulation of an Amorphous Pharmaceutical by initiated Chemical Vapor Deposition for Enhanced Stability

Paul Christian,[†] Heike M.A. Ehmman,[‡] Anna Maria Coclite,[†] and Oliver Werzer^{*‡}

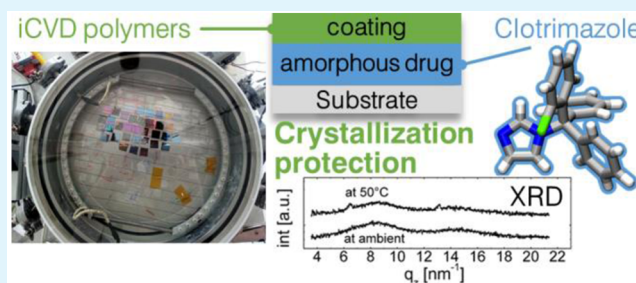
[†]Institute of Solid State Physics, NAWI Graz, Graz University of Technology, 8010 Graz, Austria

[‡]Institute of Pharmaceutical Science, Department of Pharmaceutical Technology, University of Graz, 8010 Graz, Austria

Supporting Information

ABSTRACT: The usage of amorphous solids in practical applications, such as in medication, is commonly limited by the poor long-term stability of this state, because unwanted crystalline transitions occur. In this study, three different polymeric coatings are investigated for their ability to stabilize amorphous films of the model drug clotrimazole and to protect against thermally induced transitions. For this, drop cast films of clotrimazole are encapsulated by initiated chemical vapor deposition (iCVD), using perfluorodecyl acrylate (PFDA), hydroxyethyl methacrylate (HEMA), and methacrylic acid (MAA). The iCVD technique operates under solvent-free conditions at low temperatures, thus leaving the solid state of the encapsulated layer unaffected. Optical microscopy and X-ray diffraction data reveal that at ambient conditions of about 22 °C, any of these iCVD layers extends the lifetime of the amorphous state significantly. At higher temperatures (50 or 70 °C), the p-PFDA coating is unable to provide protection, while the p-HEMA and p-MAA strongly reduce the crystallization rate. Furthermore, p-HEMA and p-MAA selectively facilitate a preferential alignment of clotrimazole and, interestingly, even suppress crystallization upon a temporary, rapid temperature increase (3 °C/min, up to 150 °C). The results of this study demonstrate how a polymeric coating, synthesized directly on top of an amorphous phase, can act as a stabilizing agent against crystalline transitions, which makes this approach interesting for a variety of applications.

KEYWORDS: clotrimazole, amorphous, iCVD, encapsulation, stabilization, X-ray diffraction, thin film, molecular arrangement



INTRODUCTION

Poor solubility and low bioavailability are major concerns in the formulation of several drug systems, limiting or even prohibiting their usage in practical application. Several approaches are known to overcome this limitation, among which particle size reduction is likely the most commonly used.¹ Besides this, the usage of the amorphous solid state is particularly appealing to the pharmaceutical formulation of poorly soluble drugs, because this state promises easier dissolution compared with the crystalline form(s).^{2–4} In the amorphous state, enhanced surface accessibility exists and lattice energies are absent, thus resulting in excess free energy.⁵ This means that the energetic barriers that molecules have to overcome in order to participate in the solubilization process are relatively low compared with those of molecules within the highly structured arrangements of a crystal. Experimental and theoretical studies have demonstrated this difference for some systems, including indomethacin^{6,7} and ritonavir.⁸ However, a significant drawback of the amorphous state is the lack of long time stability, which often results in undesired or unpredictable crystalline transition(s) over time. This makes drug formulations with amorphous active pharmaceutical ingredients challenging.⁹ The most common approach to prevent devitrification is the usage of solid dispersions, where the

amorphous active pharmaceutical component (API) is dispersed within a carrier material.^{5,10} While the definition comprises several different types of solid dispersions, it is mostly used to describe binary systems consisting of amorphous APIs within a polymeric carrier. Such systems aim to increase the glass transition temperature of the drug system because above this point enhanced molecular mobility, and thus crystallization, is facilitated.¹¹ Additionally, molecular interactions (e.g., hydrogen bonding)¹² or local entrapment within the matrix material can further stabilize the amorphous state.¹³

However, stabilization of the amorphous state through interface interactions is not limited to full encapsulation. Just the presence of a solid substrate may readily allow for enhanced stability. In the case of thin paracetamol films supported on silica surfaces, this provides stabilization up to an hour.¹⁴ For racemic ibuprofen on glass surfaces, crystallization requires more than 2 weeks, while cellulose surfaces lead to crystallite formation already within a day.¹⁵ As new formulation strategies are under development, personalized medicine might benefit from such amorphous states because the shelf life might not be

Received: May 20, 2016

Accepted: July 28, 2016

Published: July 28, 2016

the limiting parameter for successful application. Surfaces are not only capable of stabilizing amorphous states but have also the potential to facilitate crystallization into specific polymorphs or with distinct crystallographic orientations (texture). For instance, poly(3-hexylthiophene) (P3HT) assembles on a potassium 4-bromobenzoate substrate in an “edge-on” orientation.¹⁶ Single crystal surfaces induce a directed growth, which results, for instance, in *para*-sexiphenyl needles aligning along certain direction on gold or copper crystals.^{17,18} Similarly, the crystallographic orientation of caffeine needles on mica surfaces reflects the pseudo-3-fold symmetry of a complex mica sheet.^{19,20} Defined crystal growth is of high importance because polymorphic structures as well as morphologies have a tremendous impact on the physicochemical properties of a material. For drugs or pharmaceutically relevant molecules, properties such as dissolution behavior, bioavailability, and shelf life stability are of main concern. Polymorph adjustments can, for instance, induce strong changes in the drug release profile as observed in the case of chloramphenicol palmitate, in which polymorph B yields a 6 times higher maximum human plasma concentration than polymorph A.²¹ The crystallization time is another key parameter for successful application because longer production times result in more costly products. Faster crystallization rates may be facilitated by providing additional nucleation sites, such as by seeding, or by the presence of a surface in general.²² Even a combination of epitaxial growth and enhanced crystallization rates was just recently demonstrated to be effective for a carbamazepine/iminostilbene mixture.²³

Clotrimazole is commonly used in the treatment of fungal infections,²⁴ but potential application in malaria treatment²⁵ is also under research. In this study, clotrimazole is chosen as the model substance because amorphous films are easily accessible from simple solution processes such as spin coating or drop casting.²⁶ Such a system might readily be employed in different dosage forms, such as in patches for parenteral or sublingual application. Additionally, the usage of solution processes in the film preparation allows also for coprocessing clotrimazole with polymeric materials like polystyrene. This results in a solid state solution, exhibiting a strongly retarded drug release.²⁷ In general, amorphous clotrimazole films persist for several days on storage under ambient conditions. Enhanced crystallization rates result, for instance, from heat treatment or solvent vapor annealing, which lead to a variation in the crystallite morphology but leave the polymorphic form unaffected; extended spherulitic type growth, dendritic growth, or extended bar shape crystallites were observed.²⁶ In terms of practical application, such morphology alterations often result in different dissolution behavior.

Coatings of solid state drug formulations are commonly prepared by solution processes such as spray coating.²⁸ Such an approach works well for systems that do not change properties as they come into contact with solvents. However, because many drug formulations are designed to perform in aqueous environments (e.g., tablets), the application of solvents is usually limited. A solvent-free method that also allows the coating of such dosage forms is chemical vapor deposition (CVD). With this technique, polymers of defined chemical composition can be synthesized directly at, for instance, tablet surfaces. In principle, this method is applicable to any surface so that even liquid matter can be coated.²⁹ A recently developed variation of this process is initiated CVD (iCVD).³⁰ In this, primary radicals are created by thermal fragmentation of an initiator molecule (e.g., a peroxide with a labile O–O bond) at

a heated filament.³¹ The introduction of an initiator molecule lowers the energy required for radical generation so that polymerization can be performed even at low filament (usually in the range 150–300 °C) and substrate temperatures (usually below 60 °C). In turn, this promotes selective chemistry because the radicals react exclusively with the vinyl bonds of a monomer, creating an initiator–monomer radical, which itself is capable of reacting with another monomer unit. The process is propagated along chain growth until a radical site is terminated by either another initiator molecule or another active chain.^{32,33}

In recent years, this process enabled coatings with tailored properties, including thermal³⁴ or pH-responsiveness,³⁵ encapsulation,³⁶ and swellability,³⁷ among many more.

In this work, three different polymer compositions were deposited by iCVD on top of amorphous clotrimazole films to study how the stability of the drug solid state is affected: poly(2-hydroxyethyl methacrylate) [p-HEMA], poly(methacrylic acid) [p-MAA], and poly(perfluorodecyl acrylate) [p-PFDA]. Both p-HEMA and p-MAA are of interest in drug formulation because they bring distinct functionalities with them, possibly allowing for drug release only in a certain environment (e.g., acidic in the stomach). While p-MAA exhibits pH-responsiveness, p-HEMA forms a hydrogel. This means that the mesh size will increase in an aqueous environment, which should lead to enhanced drug dissolution behavior in turn. p-PFDA was chosen as a contrast to the other polymers. It exhibits crystallinity itself and is highly hydrophobic, which should, in turn, make it a perfect encapsulation, preventing any water uptake (hydrate formation can be a problem for many drugs). For practical application, also the biocompatibility of such materials has to be considered. While biocompatibility has been demonstrated for both p-HEMA^{38,39} and p-MAA⁴⁰ in several cases, there is no data for the biocompatibility of p-PFDA in literature (to our knowledge). Anyway, thorough testing will be necessary for all the compounds before such a polymer system can be used in actual medication. These polymeric encapsulation layers confine the drug film, which is then unable to crystallize at the solid–air interface. As a consequence, the coating layer introduces another solid–solid boundary. By employing investigation techniques such as optical microscopy, X-ray diffraction, or *ex situ* and *in situ* thermal treatment, the impact of these coatings on the amorphous films is studied along with how the film stability and the eventual crystallization is affected.

■ MATERIALS AND METHODS

Pharmaceutical grade clotrimazole (IUPAC name 1-[(2-chlorophenyl)(diphenyl)methyl]-1H-imidazole) was purchased from Gatt-Koller GmbH (Austria) and used without further purification. For sample preparation, a clotrimazole–tetrahydrofuran solution (Aldrich, Germany) of 60 mg/g (0.15 mol/L) was prepared. As substrates, conventional glass slides (Carl Roth GmbH+Co.KG, Germany) of 2.5 × 2.5 cm² size were sonicated in an acetone bath for 15 min, subsequently rinsed with 2-propanol and finally dried under a nitrogen stream. For sample preparation, 100 μL of the solution was drop cast onto the substrates, leveled precisely horizontally. Additionally, the samples were covered by a Petri dish, allowing for a slower and more controlled solvent evaporation, which resulted in reproducible, high quality films.

Polymer coatings of 2-hydroxyethyl methacrylate (HEMA, 97%, Aldrich, Germany), 1H,1H,2H,2H-perfluorodecyl acrylate (PFDA, 97%, Aldrich, Germany), and methacrylic acid (MAA, 99%, Aldrich, Germany) (Figure 1) were deposited in a custom-built iCVD chamber,

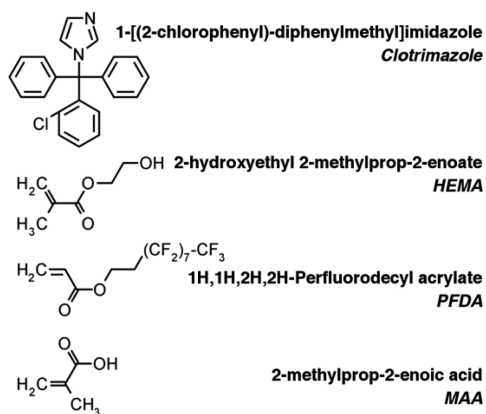


Figure 1. Structural formulas of clotrimazole and the monomers used in the iCVD process, together with the corresponding names.

using *tert*-butyl peroxide (TBPO, 98%, Aldrich, Germany) as initiator. The individual polymers are denoted as p-HEMA, p-MAA, and p-PFDA from here on. (A more detailed description is provided in the [Supporting Information](#).) Additionally, ethylene glycol dimethacrylate (EGDMA, 98%, Aldrich, Germany) was employed as cross-linking agent for p-MAA and p-HEMA. For all samples, the same coating thickness of 200 nm was deposited.

The crystalline sample properties were investigated with a PANalytical Empyrean X-ray diffractometer, equipped with a copper sealed tube (wavelength $\lambda = 0.154$ nm), a Göbbel mirror, various slits, and a PIXcel^{3D} solid state detector. The angular scans ($\theta/2\theta$) are represented in the scattering vector (q_z) notation, whereby $q_z = 4\pi \sin(\theta)/\lambda$. Such a representation allows for a direct comparison of measurements taken at other wavelengths. The index z denotes that only net-planes parallel to the substrate surface are evaluated in these particular measurements (“specular scans”). The diffuse scattering from the amorphous glass substrate is subtracted prior plotting.

To study the effect of temperature on the crystallization behavior, samples were subject to *ex situ* and *in situ* heating. *Ex situ* isothermal annealing was performed in standard ovens at 50 and 70 °C, respectively, under ambient atmosphere. *In situ* temperature-dependent X-ray diffraction measurements were performed using a DHS900 heating stage (Anton-Paar, Austria). Individual samples were heated to 170 °C, using a heating rate of 3 °C/min.

Optical images were taken on an AxioVert polarization microscope (Zeiss, Germany) with a high resolution camera. For some samples, the topographic information was recorded by a FlexAFM (Nanosurf, Switzerland) equipped with an EasyScan 2 controller. All measurements were taken in noncontact mode using Tap300 cantilevers (BudgetSensors, Bulgaria). The data were processed and depicted using the software package Gwyddion.⁴¹

RESULTS

Pristine Clotrimazole Films. Clotrimazole solutions were drop cast onto glass substrates, forming homogeneous liquid layers. Upon solvent evaporation, a solid film of several micrometers height is established in about 5 min. Such films are initially completely transparent (thus, optical data are omitted), indicating that the amorphous state is present. The X-ray diffraction exhibits, indeed, no Bragg peaks but two broad humps around $q_z \approx 8$ and 15 nm^{-1} (see [Figure 2](#)), indicative for low order within this film.

On ambient storage, the diffraction pattern changes significantly within 48 h. Multiple peaks have emerged, with the most prominent being located between $q_z = 6$ and 7 nm^{-1} . This means that the clotrimazole film has (at least partially) crystallized. A comparison with theoretical powder spectra data shows agreement with the triclinic form of clotrimazole, with

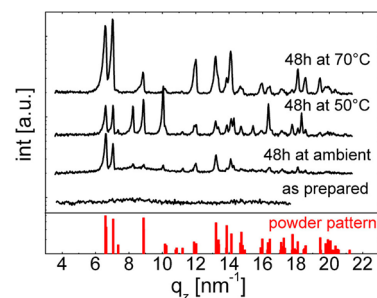


Figure 2. X-ray diffraction scans of an as-prepared clotrimazole film and films stored at different temperatures. The red bars indicate positions and the intensities of an ideal powder.

lattice parameters $a = 8.76 \text{ \AA}$, $b = 10.55 \text{ \AA}$, $c = 10.61 \text{ \AA}$, $\alpha = 114.1^\circ$, $\beta = 96.96^\circ$, and $\gamma = 97.54^\circ$.⁴² Because the peak intensities do not follow those of an ideal powder, a slight texture (i.e., favorable contact planes parallel to the surface) is present. Additional peaks are noted at $q_z = 8.25, 10.04, 14.30, 15.40,$ and 18.34 nm^{-1} , which are unexplained by the triclinic form. Because there are still two amorphous humps in the pattern, full crystallization was not achieved within the 48 h storage at ambient conditions.

The coexistence of both crystalline and amorphous clotrimazole is also apparent in the optical micrograph (see [Figure 3a](#)). Several densely packed spherulites correspond to

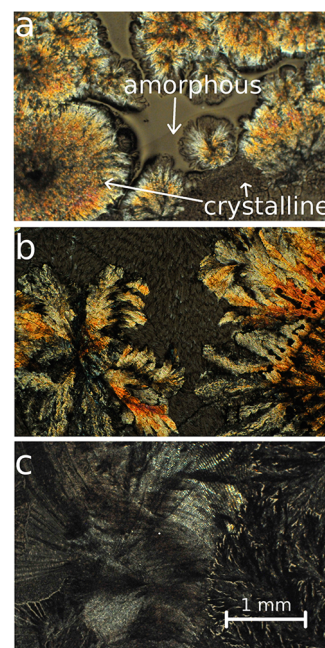


Figure 3. Optical micrographs of pristine clotrimazole films 48 h after preparation, stored at ambient temperature (a), 50 °C (b), or 70 °C (c). Arrows indicate crystalline regions as well as amorphous fractions of clotrimazole.

crystals. Within these spherulites, the color varies, likely the result of deviating thicknesses or differences in the crystal contact planes. Remaining portions of the “as-prepared” film are found. While this confirms amorphous fraction, the amount was small. Eventually, another 12–24 h storage would transfer such a partially crystalline film into a solely crystalline one.

Full crystallization results within 48 h when a film is stored at a higher temperature (50 °C). The micrograph exhibits

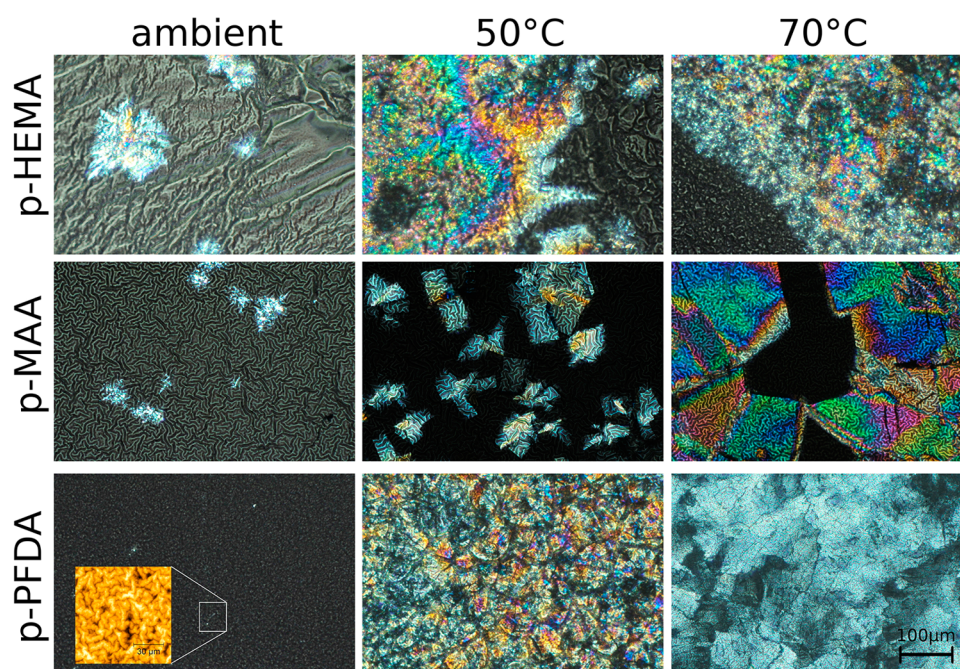


Figure 4. Various clotrimazole–iCVD samples stored for 48 h at different temperatures. The inset of the p-PFDA sample displays an AFM height image of the surface.

exclusively crystalline regions with two distinct morphologies (see Figure 3b): first bold, colorful structures branching from common centers and second, pale looking structures with random distribution. Transparent (amorphous) film portions are absent, meaning that likely all material was crystalline. In the limit of the experiment, this agrees with the X-ray scan, in which amorphous humps are absent (see Figure 2). The Bragg peak positions remained the same, although a variation in the relative intensities is noted. Peaks characteristic for the triclinic polymorph exhibit here a powder-like intensity distribution, that is, a common contact plane with the substrate is missing. But also the peaks of the unknown phase are more intense, suggesting that more crystals exist in this phase.

Sample treatment at 70 °C for 48 h resulted mainly in pale spherulitic structures (see Figure 3c). The absence of colorful features in the optical micrograph suggests similar thicknesses for these structures. Like the previous samples, the diffraction pattern displays peaks typical for the triclinic form, while peaks of the unknown phase have disappeared. Amorphous humps are also absent in this pattern; thus (in the limit of the experiment) full crystallization results for samples stored at 70 °C within 48 h.

iCVD Coatings on Amorphous Films. Amorphous clotrimazole films supported on glass substrates were coated with p-HEMA, p-MAA, or p-PFDA layers. After the iCVD deposition, the encapsulated clotrimazole remained in the amorphous state for all the samples. These samples were stored either at ambient, 50 °C, or 70 °C, for 48 h each. Then optical micrographs (Figure 4) and X-ray diffraction patterns (Figure 5) were collected. For a p-HEMA coating, two dominant features are noted. First, a strong surface wrinkling is evident. Visual inspection during the iCVD process shows that films turn opaque already within short deposition times, that is, at thin coating layer thicknesses. This means that surface wrinkling develops at early deposition stages, whereby the increase in roughness (wrinkles) causes the opaque appearance. The second interesting aspect is that for 48 h storage, the

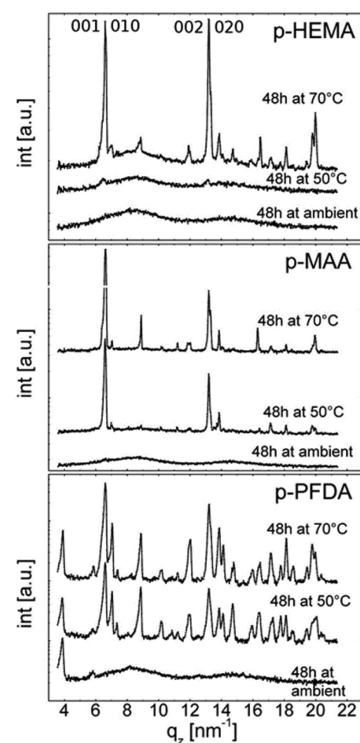


Figure 5. X-ray diffraction scans of clotrimazole encapsulated with different polymers after storage at different conditions. Images share a common abscissa for sake of comparability.

majority of the clotrimazole film remained amorphous, which appears greyish in the image. Only some crystals were present (bright areas in the image). Please note that this image does not reflect the statistic nature of the entire sample, that is, the crystalline fraction is overrepresented in this image compared with the entire sample. This agrees with the corresponding diffraction scan, which displays two amorphous humps but not

Bragg peaks. Because X-ray scans generally contain integral information on a sample (and thus are a good statistical estimate), the total number of clotrimazole crystals in the sample is likely very small.

Using storage temperatures of 50 or 70 °C, the crystalline fractions enlarged (Figure 4, top row). These crystals show more defined shapes (note that the apparent “fuzzy” surface of the crystalline regions is in fact the wrinkled polymeric top layer). The crystalline regions appear similar in shape for both samples but the number of crystals is lower when stored at 50 °C. This agrees with the X-ray results (Figure 5), which show diffraction from triclinic clotrimazole as well as scattering from amorphous fractions. Two dominant peaks are noted for both samples, located at $q_z = 6.5 \text{ nm}^{-1}$ and 13 nm^{-1} , meaning that these samples are textured. A closer inspection shows that each peak is in fact a convolution of two separate peaks (see Supporting Information), which correspond to distinct crystallographic planes, that is, the crystals contact the substrate/polymer coating preferentially along the 001 and 010 planes. On account of the low crystallinity, other peaks are absent in the 50 °C.

Samples with a p-MAA coating show a similar qualitative behavior, although differing quantitatively. The different morphologies of the samples after storage at different temperatures for 48 h appear in the optical images (Figure 4, middle row). The p-MAA coating exhibits surface wrinkling (with shorter periodicity in the wrinkles compared with the p-HEMA layer), as most evident for the sample stored at ambient. The underlying clotrimazole film remained largely in an amorphous state (greyish area), with only some crystals being present (brighter areas in the micrograph). Accordingly, the X-ray scan (Figure 5) shows solely diffraction from amorphous clotrimazole, meaning that the amount of crystals is small.

Upon 50 °C storage, a larger fraction of clotrimazole crystallized, with the shape of the individual crystals being plate-like. The strong double peak in the X-ray diffraction pattern at $q_z = 6.5 \text{ nm}^{-1}$ (and higher order reflections), corresponding to the 001 and 010 orientation, means that two preferred contact planes exist between clotrimazole and the p-MAA coating. Optical and diffraction data show that only a small fraction remained amorphous. For storage temperatures of 70 °C, the situation remains similar, only the number and size of crystals being larger.

The clotrimazole crystallization changes drastically when encapsulated by p-PFDA. After deposition, the samples retain their transparent appearance (see Figure 4, bottom left). An AFM image (inset in Figure 4, bottom left) shows a sample surface after being stored for 48 h at ambient, which clearly hosts wrinkles. However, compared with the other samples, the wrinkles are of much smaller lengths and heights. This sample also lacks crystalline clotrimazole, demonstrating the capability of p-PFDA coating of preventing (or at least retarding) clotrimazole crystallization under ambient conditions. The X-ray diffraction pattern in Figure 5 features two peaks and two broad humps. The sharp peaks located at $q_z = 3.86$ and 5.79 nm^{-1} are higher order reflections of the lamellar packing with the fluorine groups of the p-PFDA (d -spacing $\approx 3.25 \text{ nm}$) exhibiting parallel stacking onto the sample.⁴³ The two broad humps are solely attributed to amorphous clotrimazole.

Upon storage at higher temperatures (50 or 70 °C), the amorphous clotrimazole transfers into the crystal state. The optical data shows the formation of extended plate-like

crystallites similar to the p-MAA sample. The X-ray pattern, however, reveals the absence of a defined clotrimazole contact plane when coated with p-PFDA. The diffraction pattern resembles more that of an ideal powder, in which any order in respect to the substrate surface is completely absent.

In Situ Heating of Amorphous Films. To follow the structural evolution on temperature change, clotrimazole layers with and without polymeric encapsulation were investigated using *in situ* X-ray diffraction experiments. The evolution of the diffraction patterns as a function of temperature is summarized in Figure 6 for the various samples. For a bare clotrimazole

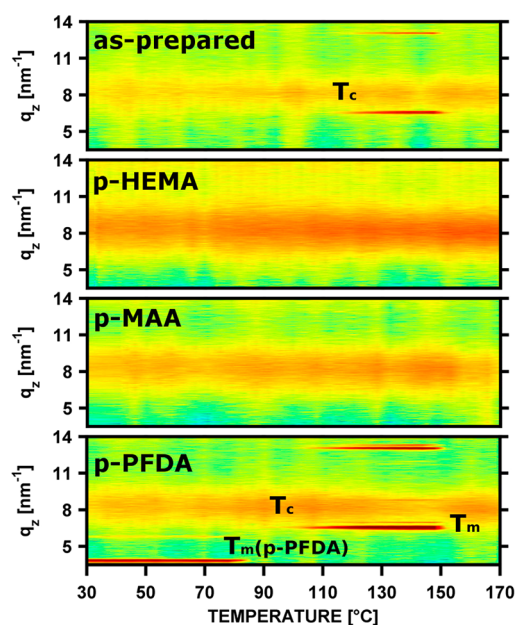


Figure 6. *In situ* X-ray diffraction scans of amorphous clotrimazole films, encapsulated by iCVD layers, at different temperatures. T_c and T_m denote the onset of clotrimazole crystallization and melting, respectively. $T_{m(p-PFDA)}$ denotes melting of the p-PFDA lamella.

layer, that is, without coating, the diffraction data contains initially information from the amorphous film. A moderate elevation of the temperature had no impact. Reaching 108 °C, crystallization was initiated and the 001/010 double peak started to evolve at $q_z = 6.57 \text{ nm}^{-1}$. The peak intensity increased steadily up to 148 °C, meaning that the amount of crystals is likewise increasing. Though hardly visible, also other peaks emerged, for example, at $q_z = 7.0 \text{ nm}^{-1}$, meaning also crystals with other contact planes start to grow, similar to the behavior observed in isothermal heat treatments. Exceeding 150 °C, the intensities decreased on account of clotrimazole melting. It is noteworthy that the amorphous state prevails on rapid cooling ($>50 \text{ °C/min}$), so that crystallization experiments can eventually be repeated.

Samples hosting polymer coatings of p-HEMA or p-MAA showed different temperature responses. Over the course of the experiments, sharp peaks, as present for the pristine clotrimazole, were absent and only the broad amorphous humps persisted. The polymeric coating thus fully suppresses clotrimazole crystallization for short temperature increases up to the melting point of crystalline clotrimazole, that is, 150 °C.

The initial pattern of the clotrimazole–p-PFDA sample contains two sharp peaks at $q_z = 3.86$ and 5.79 nm^{-1} , characteristic of the p-PFDA lamella order, as well as the

amorphous clotrimazole hump. This pattern prevails unaffected until 80 °C, at which the two peaks disappeared. At this temperature p-PFDA melts. On a further temperature increase to 92 °C, the 001 double peak of clotrimazole at $q_z = 6.57 \text{ nm}^{-1}$ emerges. This crystallization onset temperature is significant lower compared with the unprotected sample. On further heating, more material crystallized as evident by the higher peak intensity. Besides the strong 001 peak, there are also other peaks present, meaning that also crystallization in arbitrary directions took place and thus, a powder-like behavior resulted, with no (or only a slight) texture. At a temperature of 150 °C, the crystalline clotrimazole melts, which agrees with the uncoated sample.

DISCUSSION

Clotrimazole consists of four rings joined together and is of rather asymmetric and bulky shape (Figure 1), which generally results in slower crystallization dynamics. Thin clotrimazole films require more than 48 h to transit from an amorphous into a crystalline state, at least when stored in ambient conditions and hosted on glass. In comparison, amorphous phenytoin thin films require only some minutes until the first crystals start forming.⁴⁴ Nevertheless, the clotrimazole crystallization rate increases as elevated storage temperatures are employed; high temperatures facilitate in general diffusion of molecules both on interfaces and in the bulk. Already at 50 °C, which is about 1/3 of the melting temperature, significantly more crystals develop. The better diffusion capabilities allow molecules to adapt faster to adjacent molecules, thus fostering nuclei formation or adsorption at crystalline sites. The optical microscopy shows spherulitic structures with growth from arbitrary directions (confirmed by X-ray experiments), that is, neither the organic–glass nor the solid–air interface can dictate selective growth from specific contact planes. The presence of spherulite centers mean common crystal initiation sites are present. These sites, however, are unable to grow into larger crystals. This is also likely caused by limited diffusion in the solid state, and thus diffusion limited growth mode of branching spherulitic arms is expected.

The amorphous clotrimazole state is robust and persists throughout the iCVD deposition. In addition, clotrimazole does not sublimate under moderate vacuum conditions and the substrate temperature of 30 °C used. Similarly, other drugs like indomethacin or phenytoin can be encapsulated by this route, while other active pharmaceutical ingredients like caffeine, paracetamol, or ibuprofen are prone to sublimation. In general, the iCVD process performs well in a wide range of different temperatures and pressures, which might enable using these encapsulations also for such volatile materials.

The encapsulation of the amorphous drug exhibits surface wrinkling in the polymeric layer. The p-HEMA layer resulted in pronounced wrinkles of several micrometers extension. p-MAA produces less pronounced wrinkles, while wrinkles in p-PFDA coating are much smaller, which (compared with the other cases) seems negligible. Often, wrinkling is a result of two materials having different physicochemical properties. Especially differences in elastic moduli (E) of a “substrate” (here the clotrimazole layer) and the coating explain wrinkling. Depending on the theory for calculation, the wrinkling amplitude (A) might follow $A \approx E^{1/3}$.⁴⁵ From this, it is estimated that p-HEMA is the softest material while p-PFDA is the stiffest, with the E of p-MAA being between these two. This assumption is also in agreement with literature data on such films, reporting

an elastic modulus of 183 MPa for p-HEMA and one of 8.2 GPa for p-PFDA.^{46,47} A test shows that such wrinkling is absent in coatings of crystalline clotrimazole layers (an example is shown in the Supporting Information). After heating such samples to the melting point of clotrimazole (150 °C), wrinkles formed again. Surprisingly, cooling or a subsequent crystallization did not change the morphology of surface wrinkles. This means that surface “relaxation” deformed the surface, but crystallization does not cause additional strain so that wrinkling remained unchanged. As will be shown elsewhere, the size of the wrinkling structures also correlates with the thickness of the clotrimazole layer between the substrate and the iCVD layers. For sake of faster dissolution, wrinkled surfaces might be favorable because the accessible surface areas are larger compared with a flat surface. Especially the usage of p-HEMA with its capability to swell in an aqueous environment might allow for very controlled release.

The deposition of coating layers on top of an amorphous clotrimazole film results in an alteration of the clotrimazole crystallization. While uncoated samples crystallize within 48 h, coated samples stored at ambient conditions remain amorphous significantly longer. p-PFDA coatings did not show any indication of clotrimazole crystallization and only a very small number of crystals formed under p-HEMA and p-MAA coatings. The reason for this behavior cannot unambiguously be identified. However, the exchange of the solid–air interface by another solid–solid interface (i.e., clotrimazole–iCVD coating) strongly hinders the molecular movement at this interface. This means that the probability of nuclei formation and thus also of crystal growth drastically reduces. The drug molecules remain longer in their respective spatial positions, and the amorphous state prevails.

At temperatures higher than ambient, the iCVD layers cannot fully suppress crystallization. Interestingly, the p-PFDA layer shows protection at ambient temperatures, but it is unable to prevent crystallization at 50 or 70 °C. Also a rapid heat increase causes the amorphous clotrimazole to crystallize. Because p-PFDA surfaces are strongly hydrophobic and oleophobic,⁴⁸ most substances prevent contact, meaning surface diffusion eases because solid–solid interface interaction strengths are small. Furthermore, the formation of various crystallographic orientations means that crystallization in arbitrary directions takes place, which agrees with the assumption of poor interactions. It can be concluded that p-PFDA coatings result in clotrimazole films behaving similar to an uncoated sample, with similar crystallization times and undirected growth.

In contrast, p-HEMA and p-MAA layers are more effective in suppressing crystallization, which, independent of the storage temperatures, provides large amounts of amorphous clotrimazole even after 48h storage. Noteworthy, they prevent clotrimazole crystallization even through brief heat treatments up to the melting point of crystalline clotrimazole. This is of high practical interest, since, for instance, sterilizing processes often need heat treatments, which puts amorphous drug formulations at risk of crystallization. The pH-responsiveness of p-MAA or the hydrogel properties of p-HEMA would possibly allow for an encapsulation design with an environment-sensitive or retarded release, respectively. Also the usage of these polymers as matrix material for drug loading is possible. For practical application, thin film administration routes (such as buccally or sublingually) seem to be the natural choice, given the sample design used in this study. But also whole tablets can

be encapsulated by the iCVD technique, making this technique broadly applicable. Whether the polymer should be part of the final drug formulation has to be decided on a case to case basis, requiring additional testing of biocompatibility, permeability, and chemical and physical stability of the polymer. Eventually, slower heating ramps, that is, less than 3 °C/min, would allow induction of crystallization also in these samples in one heat run.

p-HEMA or p-MAA layers result in a more defined crystallization compared with the other samples. Clotrimazole crystals align preferentially along two specific crystallographic planes with the polymer/substrate interface, as illustrated in Figure 7. In the 001 orientation, the contact at the solid–solid

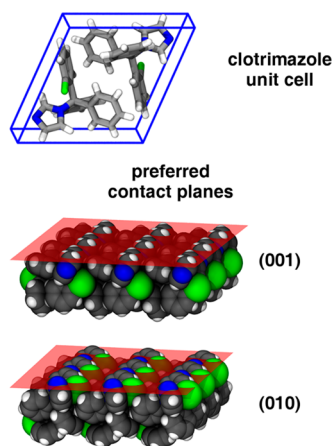


Figure 7. Molecular packing in the clotrimazole unit cell (top) and the two preferred molecular contact planes between clotrimazole crystals and the p-HEMA and p-MAA encapsulation layers (bottom); the structures are illustrated with the software package VMD.⁴⁹

interface is mostly facilitated by the apolar C–H groups, with the polarizable chloric unit embedded within the bulk. Nevertheless, also some polar interactions with the –OH groups of the polymers might be present in this configuration, because the nitrogen in the imidazole ring (i.e., the hydrogen bond acceptor side) is in close proximity to the interface. The polar interaction becomes more dominant in the 010 assembly, since there the hydrogen bond acceptor sides (and the chloric unit) are directly exposed at the interface. The presence of the two preferred crystallographic orientations in clotrimazole means that the molecules near the polymer–drug interface need to adapt their conformation (rotation and translation) in order to adsorb or physisorb at this interface. Because this is time-consuming, nucleation or condensation at lattice sites is less likely to occur, extending therefore the lifespan of the amorphous phase. This agrees with the observation that elevated temperatures accelerate crystal growth within such films.

CONCLUSION

The solid state transition from amorphous to crystalline clotrimazole films can be strongly altered by modifying the drug–air interface through a polymer encapsulation. The use of a solvent-free process (i.e., iCVD) in the deposition of the polymer layer circumvents any risk of solvent-induced solid state transitions in the drug or dissolution. Three different iCVD encapsulating layers were investigated: p-PFDA, p-MAA, and p-HEMA. Each of these layers stabilized the drug in its

amorphous state. At higher temperatures, the protection failed in the case of p-PFDA, while both the p-HEMA and the p-MAA encapsulations reduced the crystallization rate significantly. Furthermore, the chemical composition of the polymer layers also enables selective growth so that clotrimazole crystallites contact the polymer layers along the (001) and (010) planes, on account of both apolar interaction forces and hydrogen bonding. Suppressing crystallization upon a rapid temperature increase makes this encapsulation interesting for application relevant processes such as sterilization, where high temperatures are only briefly required. While this study is limited to only three different polymers, the general applicability of such an iCVD encapsulating layer to drug molecules motivates this approach for other polymeric compositions, which might then enable further tuning of the crystallization behavior.

ASSOCIATED CONTENT

Supporting Information

The Supporting Information is available free of charge on the ACS Publications website at DOI: 10.1021/acsami.6b06015.

Description of the iCVD setup and the deposition conditions, detailed view of the XRD pattern of p-HEMA encapsulated clotrimazole, optical microscopy of the wrinkling in p-HEMA (PDF)

AUTHOR INFORMATION

Corresponding Author

*E-mail: oliver.werzer@uni-graz.at.

Notes

The authors declare no competing financial interest.

ACKNOWLEDGMENTS

The work was funded by the Austrian Science Fund (FWF) [Grant P25541-N19]. The authors thank the NAWI Graz for support. Part of the research was supported by a Marie Curie International Incoming Fellowship (Project 626889) within the 7th European Community Framework Programme.

REFERENCES

- (1) Kesisoglou, F.; Panmai, S.; Wu, Y. Nanosizing — Oral Formulation Development and Biopharmaceutical Evaluation. *Adv. Drug Delivery Rev.* **2007**, *59* (7), 631–644.
- (2) Hancock, B. C.; Parks, M. What Is the True Solubility Advantage for Amorphous Pharmaceuticals? *Pharm. Res.* **2000**, *17* (4), 397–404.
- (3) Yu, L. Amorphous Pharmaceutical Solids: Preparation, Characterization and Stabilization. *Adv. Drug Delivery Rev.* **2001**, *48* (1), 27–42.
- (4) Babu, N. J.; Nangia, A. Solubility Advantage of Amorphous Drugs and Pharmaceutical Cocrystals. *Cryst. Growth Des.* **2011**, *11* (7), 2662–2679.
- (5) Kaushal, A. M.; Gupta, P.; Bansal, A. K. Amorphous Drug Delivery Systems: Molecular Aspects, Design, and Performance. *Crit. Rev. Ther. Drug Carrier Syst.* **2004**, *21* (3), 133–193.
- (6) Imaizumi, H.; Nambu, N.; Nagai, T. Stability and Several Physical Properties of Amorphous and Crystalline Forms of Indomethacin. *Chem. Pharm. Bull.* **1980**, *28* (9), 2565–2569.
- (7) Murdande, S. B.; Pikal, M. J.; Shanker, R. M.; Bogner, R. H. Solubility Advantage of Amorphous Pharmaceuticals: I. A Thermodynamic Analysis. *J. Pharm. Sci.* **2010**, *99* (3), 1254–1264.
- (8) Law, D.; Schmitt, E. A.; Marsh, K. C.; Everitt, E. A.; Wang, W.; Fort, J. J.; Krill, S. L.; Qiu, Y. Ritonavir-PEG 8000 Amorphous Solid Dispersions: In Vitro and in Vivo Evaluations. *J. Pharm. Sci.* **2004**, *93* (3), 563–570.

- (9) Hancock, B. C.; Zografi, G. Characteristics and Significance of the Amorphous State in Pharmaceutical Systems. *J. Pharm. Sci.* **1997**, *86* (1), 1–12.
- (10) Van den Mooter, G. The Use of Amorphous Solid Dispersions: A Formulation Strategy to Overcome Poor Solubility and Dissolution Rate. *Drug Discovery Today: Technol.* **2012**, *9* (2), e79–e85.
- (11) Yoshioka, M.; Hancock, B. C.; Zografi, G. Crystallization of Indomethacin from the Amorphous State below and above Its Glass Transition Temperature. *J. Pharm. Sci.* **1994**, *83* (12), 1700–1705.
- (12) Taylor, L. S.; Zografi, G. Spectroscopic Characterization of Interactions Between PVP and Indomethacin in Amorphous Molecular Dispersions. *Pharm. Res.* **1997**, *14* (12), 1691–1698.
- (13) Pokharkar, V. B.; Mandpe, L. P.; Padamwar, M. N.; Ambike, A. A.; Mahadik, K. R.; Paradkar, A. Development, Characterization and Stabilization of Amorphous Form of a Low Tg Drug. *Powder Technol.* **2006**, *167* (1), 20–25.
- (14) Ehmman, H. M. A.; Werzer, O. Surface Mediated Structures: Stabilization of Metastable Polymorphs on the Example of Paracetamol. *Cryst. Growth Des.* **2014**, *14* (8), 3680–3684.
- (15) Kellner, T.; Ehmman, H. M. A.; Schrank, S.; Kunert, B.; Zimmer, A.; Roblegg, E.; Werzer, O. Crystallographic Textures and Morphologies of Solution Cast Ibuprofen Composite Films at Solid Surfaces. *Mol. Pharmaceutics* **2014**, *11* (11), 4084–4091.
- (16) Brinkmann, M. Structure and Morphology Control in Thin Films of Regioregular poly(3-Hexylthiophene). *J. Polym. Sci., Part B: Polym. Phys.* **2011**, *49* (17), 1218–1233.
- (17) Haber, T.; Muellegger, S.; Winkler, A.; Resel, R. Temperature-Induced Epitaxial Growth Modes of Para-Sexiphenyl on Au(111). *Phys. Rev. B: Condens. Matter Mater. Phys.* **2006**, *74* (4), 045419.
- (18) Oehzelt, M.; Grill, L.; Berkebile, S.; Koller, G.; Netzer, F. P.; Ramsey, M. G. The Molecular Orientation of Para-Sexiphenyl on Cu(110) and Cu(110) p(2 × 1)O. *ChemPhysChem* **2007**, *8* (11), 1707–1712.
- (19) Röthel, C.; Radziown, M.; Resel, R.; Zimmer, A.; Simbrunner, C.; Werzer, O. Complex Behavior of Caffeine Crystallites on Muscovite Mica Surfaces. *Cryst. Growth Des.* **2015**, *15* (9), 4563–4570.
- (20) Werzer, O.; Kunert, B.; Roblegg, E.; Zimmer, A.; Oehzelt, M.; Resel, R. Surface Induced Order of Solution Processed Caffeine Needles on Silica and Muscovite Mica. *Cryst. Growth Des.* **2013**, *13* (3), 1322–1328.
- (21) Aguiar, A. J.; Krc, J.; Kinkel, A. W.; Samyn, J. C. Effect of Polymorphism on the Absorption of Chloramphenicol from Chloramphenicol Palmitate. *J. Pharm. Sci.* **1967**, *56* (7), 847–853.
- (22) Diao, Y.; Myerson, A. S.; Hatton, T. A.; Trout, B. L. Surface Design for Controlled Crystallization: The Role of Surface Chemistry and Nanoscale Pores in Heterogeneous Nucleation. *Langmuir* **2011**, *27* (9), 5324–5334.
- (23) Christian, P.; Röthel, C.; Tazreiter, M.; Zimmer, A.; Salzmann, I.; Resel, R.; Werzer, O. Crystallization of Carbamazepine in Proximity to Its Precursor Iminostilbene and a Silica Surface. *Cryst. Growth Des.* **2016**, *16* (5), 2771–2778.
- (24) Sawyer, P. R.; Brogden, R. N.; Pinder, K. M.; Speight, T. M.; Avery, G. S. Clotrimazole: A Review of Its Antifungal Activity and Therapeutic Efficacy. *Drugs* **1975**, *9* (6), 424–447.
- (25) Huy, N. T.; Kamei, K.; Kondo, Y.; Serada, S.; Eanaori, K.; Takano, R.; Tajima, K.; Hara, S. Effect of Antifungal Azoles on the Heme Detoxification System of Malarial Parasite. *J. Biochem.* **2002**, *131* (3), 437–444.
- (26) Ehmman, H. M. A.; Zimmer, A.; Roblegg, E.; Werzer, O. Morphologies in Solvent-Annealed Clotrimazole Thin Films Explained by Hansen-Solubility Parameters. *Cryst. Growth Des.* **2014**, *14* (3), 1386–1391.
- (27) Ehmman, H. M. A.; Winter, S.; Griesser, T.; Keimel, R.; Schrank, S.; Zimmer, A.; Werzer, O. Dissolution Testing of Hardly Soluble Materials by Surface Sensitive Techniques: Clotrimazole from an Insoluble Matrix. *Pharm. Res.* **2014**, *31* (10), 2708–2715.
- (28) Ré, M.-I. Formulating Drug Delivery Systems by Spray Drying. *Drying Technol.* **2006**, *24* (4), 433–446.
- (29) Bradley, L. C.; Gupta, M. Encapsulation of Ionic Liquids within Polymer Shells via Vapor Phase Deposition. *Langmuir* **2012**, *28* (27), 10276–10280.
- (30) Coclite, A. M.; Howden, R. M.; Borrelli, D. C.; Petruczuk, C. D.; Yang, R.; Yagüe, J. L.; Ugur, A.; Chen, N.; Lee, S.; Jo, W. J.; Liu, A.; Wang, X.; Gleason, K. K. 25th Anniversary Article: CVD Polymers: A New Paradigm for Surface Modification and Device Fabrication. *Adv. Mater.* **2013**, *25* (38), 5392–5423.
- (31) Mao, Y.; Gleason, K. K. Hot Filament Chemical Vapor Deposition of Poly(glycidyl Methacrylate) Thin Films Using Tert-Butyl Peroxide as an Initiator. *Langmuir* **2004**, *20* (6), 2484–2488.
- (32) Lau, K. K. S.; Gleason, K. K. Initiated Chemical Vapor Deposition (iCVD) of Poly(alkyl Acrylates): A Kinetic Model. *Macromolecules* **2006**, *39* (10), 3695–3703.
- (33) Lau, K. K. S.; Gleason, K. K. Initiated Chemical Vapor Deposition (iCVD) of Poly(alkyl Acrylates): An Experimental Study. *Macromolecules* **2006**, *39* (10), 3688–3694.
- (34) McInnes, S. J. P.; Szili, E. J.; Al-Bataineh, S. A.; Vasani, R. B.; Xu, J.; Alf, M. E.; Gleason, K. K.; Short, R. D.; Voelcker, N. H. Fabrication and Characterization of a Porous Silicon Drug Delivery System with an Initiated Chemical Vapor Deposition Temperature-Responsive Coating. *Langmuir* **2016**, *32* (1), 301–308.
- (35) Lau, K. K. S.; Gleason, K. K. Particle Functionalization and Encapsulation by Initiated Chemical Vapor Deposition (iCVD). *Surf. Coat. Technol.* **2007**, *201* (22–23), 9189–9194.
- (36) Lau, K. K. S.; Gleason, K. K. Particle Surface Design Using an All-Dry Encapsulation Method. *Adv. Mater.* **2006**, *18* (15), 1972–1977.
- (37) Mari-Buyé, N.; O’Shaughnessy, S.; Colominas, C.; Semino, C. E.; Gleason, K. K.; Borrós, S. Functionalized, Swellable Hydrogel Layers as a Platform for Cell Studies. *Adv. Funct. Mater.* **2009**, *19* (8), 1276–1286.
- (38) Bose, R. K.; Lau, K. K. S. Initiated CVD of Poly(2-Hydroxyethyl Methacrylate) Hydrogels: Synthesis, Characterization and In-Vitro Biocompatibility. *Chem. Vap. Deposition* **2009**, *15* (4–6), 150–155.
- (39) Hsiue, G.-H.; Guu, J.-A.; Cheng, C.-C. Poly(2-hydroxyethyl methacrylate) film as a drug delivery system for pilocarpine. *Biomaterials* **2001**, *22*, 1763–1769.
- (40) Bajpai, S. K.; Singh, S. Analysis of Swelling Behavior of Poly(methacrylamide-Co-Methacrylic Acid) Hydrogels and Effect of Synthesis Conditions on Water Uptake. *React. Funct. Polym.* **2006**, *66* (4), 431–440.
- (41) Nečas, D.; Klapetek, P. Gwyddion: An Open-Source Software for SPM Data Analysis. *Cent. Eur. J. Phys.* **2012**, *10* (1), 181–188.
- (42) Song, H.; Shin, H.-S. The Antifungal Drug Clotrimazole. *Acta Crystallogr., Sect. C: Cryst. Struct. Commun.* **1998**, *54* (11), 1675–1677.
- (43) Coclite, A. M.; Shi, Y.; Gleason, K. K. Controlling the Degree of Crystallinity and Preferred Crystallographic Orientation in Poly-Perfluorodecylacrylate Thin Films by Initiated Chemical Vapor Deposition. *Adv. Funct. Mater.* **2012**, *22* (10), 2167–2176.
- (44) Ehmman, H. M. A.; Kellner, T.; Werzer, O. Non-Contact-Mode AFM Induced versus Spontaneous Formed Phenytoin Crystals: The Effect of Layer Thickness. *CrystEngComm* **2014**, *16* (23), 4950–4954.
- (45) Bowden, N.; Brittain, S.; Evans, A. G.; Hutchinson, J. W.; Whitesides, G. M. Spontaneous Formation of Ordered Structures in Thin Films of Metals Supported on an Elastomeric Polymer. *Nature* **1998**, *393* (6681), 146–149.
- (46) Yin, J.; Yagüe, J. L.; Eggenspieler, D.; Gleason, K. K.; Boyce, M. C. Deterministic Order in Surface Micro-Topologies through Sequential Wrinkling. *Adv. Mater.* **2012**, *24* (40), 5441–5446.
- (47) Sojoudi, H.; McKinley, G. H.; Gleason, K. K. Linker-Free Grafting of Fluorinated Polymeric Cross-Linked Network Bilayers for Durable Reduction of Ice Adhesion. *Mater. Horiz.* **2015**, *2* (1), 91–99.
- (48) Coclite, A. M.; Shi, Y.; Gleason, K. K. Grafted Crystalline Poly-Perfluoroacrylate Structures for Superhydrophobic and Oleophobic Functional Coatings. *Adv. Mater.* **2012**, *24* (33), 4534–4539.
- (49) Humphrey, W.; Dalke, A.; Schulten, K. VMD: Visual Molecular Dynamics. *J. Mol. Graphics* **1996**, *14* (1), 33–38.